

## CONTINUOUS SOLID-SOLUTION BETWEEN MERCURIAN GIRAUDITE AND HAKITE

HANS-JÜRGEN FÖRSTER<sup>§</sup> AND DIETER RHEDE

*GeoForschungsZentrum Potsdam, Telegrafenberg, D-14473 Potsdam, Germany*

GERHARD TISCHENDORF

*Bautzner Str. 16, D-02763 Zittau, Germany*

### ABSTRACT

Among the minerals of the selenide assemblage at the Niederschlema–Alberoda uranium deposit, Erzgebirge, Germany, members of the mercurian giraudite–hakite solid solution intergrown with berzelianite and galena have been identified as rare and previously unknown phases. They form complexly zoned, anhedral, minute (<350 μm) grains embedded in a dolomite matrix. Compositional variability is expressed by the following crystallochemical formula (calculated on the basis of 29 atoms per formula unit):  $(\text{Cu}_{9.92-9.99}\text{Ag}_{0.01-0.08})\Sigma_{10.00}(\text{Hg}_{0.92-1.81}\text{Cu}_{0.06-1.12}\text{Zn}_{0.05-0.10}\text{Fe}_{0.00-0.15})\Sigma_{1.98-2.06}(\text{As}_{0.69-3.98}\text{Sb}_{0.02-3.29})\Sigma_{3.91-4.08}(\text{Se}_{10.47-11.53}\text{S}_{1.47-2.61})\Sigma_{12.90-13.09}$ . The solid solutions span the range from  $\text{gir}_{99.5}\text{hak}_{0.5}$  to  $\text{gir}_{16.2}\text{hak}_{83.8}$ , suggesting complete miscibility between mercurian giraudite and mercurian hakite in nature, equivalent to what already has been established for their S-bearing analogues, tennantite and tetrahedrite. The lack of thermodynamic data for both Se-rich species limits reliable inferences on the P–T–X conditions that prevailed during their formation. The assemblage mercurian giraudite–hakite + berzelianite + galena may represent a short-term equilibrium paragenesis of Jurassic age, formed at temperatures between 110 and 150°C under the conditions of low Se and S activities (*i.e.*,  $-26 < \log f(\text{Se}_2) < -31$  and  $-24 < \log f(\text{S}_2) < -28$  at ~110°C), before the bulk of the selenide minerals crystallized. A second, less likely hypothesis calls upon the formation of the mercurian giraudite–hakite solid solutions during an early Cretaceous event, when pre-existing selenide minerals (berzelianite) were partially attacked by infiltrating fluids that introduced the major portion of the As and Sb into the system.

**Keywords:** giraudite, hakite, mercury, selenium minerals, solid solution, miscibility, uranium deposit, Schlema–Alberoda, Erzgebirge, Germany.

### SOMMAIRE

Parmi les minéraux de l'assemblage de séléniures présents au gisement d'uranium de Niederschlema–Alberoda, Erzgebirge, en Allemagne, se trouvent des membres de la solution solide giraudite–hakite riche en mercure, en intercroissance avec berzélianite et galène. Les membres de la solution solide, espèces rares et méconnues, forment de petits (<350 μm) grains xénomorphes zonés de façon complexe dans une matrice dolomitique. La variabilité chimique est bien rendue par la formule cristallochimique suivante, calculée sur une base de 29 atomes par unité formulaire:  $(\text{Cu}_{9.92-9.99}\text{Ag}_{0.01-0.08})\Sigma_{10.00}(\text{Hg}_{0.92-1.81}\text{Cu}_{0.06-1.12}\text{Zn}_{0.05-0.10}\text{Fe}_{0.00-0.15})\Sigma_{1.98-2.06}(\text{As}_{0.69-3.98}\text{Sb}_{0.02-3.29})\Sigma_{3.91-4.08}(\text{Se}_{10.47-11.53}\text{S}_{1.47-2.61})\Sigma_{12.90-13.09}$ . Ces compositions vont donc de  $\text{gir}_{99.5}\text{hak}_{0.5}$  à  $\text{gir}_{16.2}\text{hak}_{83.8}$ , ce qui laisse supposer qu'il y a miscibilité complète entre giraudite et hakite mercurielles dans la nature, comme c'est le cas pour leurs analogues à dominance de soufre, tennantite et tétraédrite. Le manque de données thermodynamiques pour les espèces riches en Se élimine la possibilité de déduire les conditions P–T–X pendant leur formation. L'assemblage giraudite–hakite mercurielles + berzélianite + galène pourrait représenter une paragenèse stable pour un bref intervalle à l'époque jurassique, entre 110 et 150°C, sous conditions de faibles activités en Se et S (*i.e.*,  $-26 < \log f(\text{Se}_2) < -31$  et  $-24 < \log f(\text{S}_2) < -28$  à ~110°C), avant la formation des séléniures plus communs. Selon une seconde hypothèse, jugée moins probable, les membres de la solution solide giraudite–hakite mercurielles se seraient formés lors d'un événement crétacé précoce, quand les séléniures précurseurs, dont la berzélianite, se sont vus partiellement dissous lors de l'infiltration d'une phase fluide qui a introduit la plus grande partie de l'arsenic et de l'antimoine dans le système.

(Traduit par la Rédaction)

**Mots-clés:** giraudite, hakite, mercure, minéraux de sélénium, solution solide, miscibilité, gisement d'uranium, Schlema–Alberoda, Erzgebirge, Allemagne.

<sup>§</sup> *Present address:* Institute of Earth Sciences, University of Potsdam, P.O. Box 601553, D-14415 Potsdam, Germany. *E-mail address:* for@geo.uni-potsdam.de

## INTRODUCTION

Selenide-bearing hydrothermal deposits occur mainly in four environments (Simon *et al.* 1997): (1) telethermal selenide vein-type deposits, (2) unconformity-related vein-type uranium deposits, (3) sandstone-hosted uranium deposits, and (4) epithermal Au–Ag deposits in subaerial volcanic environments. Reports on selenide minerals associated with uranium deposits are numerous (*e.g.*, Coleman & Delavaux 1957, Seeliger & Strunz 1965, Brodin 1967, Harris *et al.* 1970, Ruhlmann *et al.* 1980, Dill 1981, Johan *et al.* 1982, Cabri *et al.* 1991, Zheng *et al.* 1993, Ledeneva & Pakul'nis 1997). The western Erzgebirge metallogenic province of Germany is one of the regions in which selenide minerals are associated with unconformity-related uranium deposits.

The Niederschlema–Alberoda uranium ore deposit in the Schneeberg – Schlema–Alberoda ore district is the major selenide occurrence in the Erzgebirge (Fig. 1). The first detailed mineralogical and paragenetic studies of the selenide assemblages in the 1960s and 1970s (Harlass & Schützel 1965, Ryschow 1972) were later

supplemented with electron-microprobe studies performed by Russian investigators (*e.g.*, Dymkov *et al.* 1982, 1989, 1991).

Selenide minerals occur mainly as nests (2–5 cm in diameter) and fracture fillings in dolomite – ankerite – calcite veins, or they are disseminated in intergranular spaces in the Fe–Mg carbonates. The Se minerals reported from Schlema–Alberoda (Harlass & Schützel 1965, Ryschow 1972, Dymkov *et al.* 1982, 1991, Förster & Tischendorf 2001) include: clausthalite (PbSe), tiemannite (HgSe), naumannite (Ag<sub>2</sub>Se), kloekmannite (CuSe), umangite (Cu<sub>3</sub>Se<sub>2</sub>), berzelianite (Cu<sub>2-x</sub>Se), bukovite (Cu<sub>3</sub>FeTi<sub>2</sub>Se<sub>4</sub>), permingeatite (Cu<sub>3</sub>SbSe<sub>4</sub>), crookesite (Cu<sub>7</sub>TiSe<sub>4</sub>), and eucairite (AgCuSe). Minerals recognized from optical properties, but not yet confirmed, include agularite (Ag<sub>4</sub>SeS), laitarcarite (Bi<sub>4</sub>Se<sub>2</sub>S), guanajuatite [Bi<sub>2</sub>(Se,S)<sub>3</sub>], stilleite (ZnSe), and eskebornite (CuFeSe<sub>2</sub>).

Schlema–Alberoda is the type locality (and until now the only occurrence) of mgriite, a Cu–As selenide of composition (Cu,Fe)<sub>3</sub>AsSe<sub>3</sub> (Dymkov *et al.* 1982, 1991). Moreover, Dymkov *et al.* (1989) described the presence of a bismuth-rich selenide considered to be

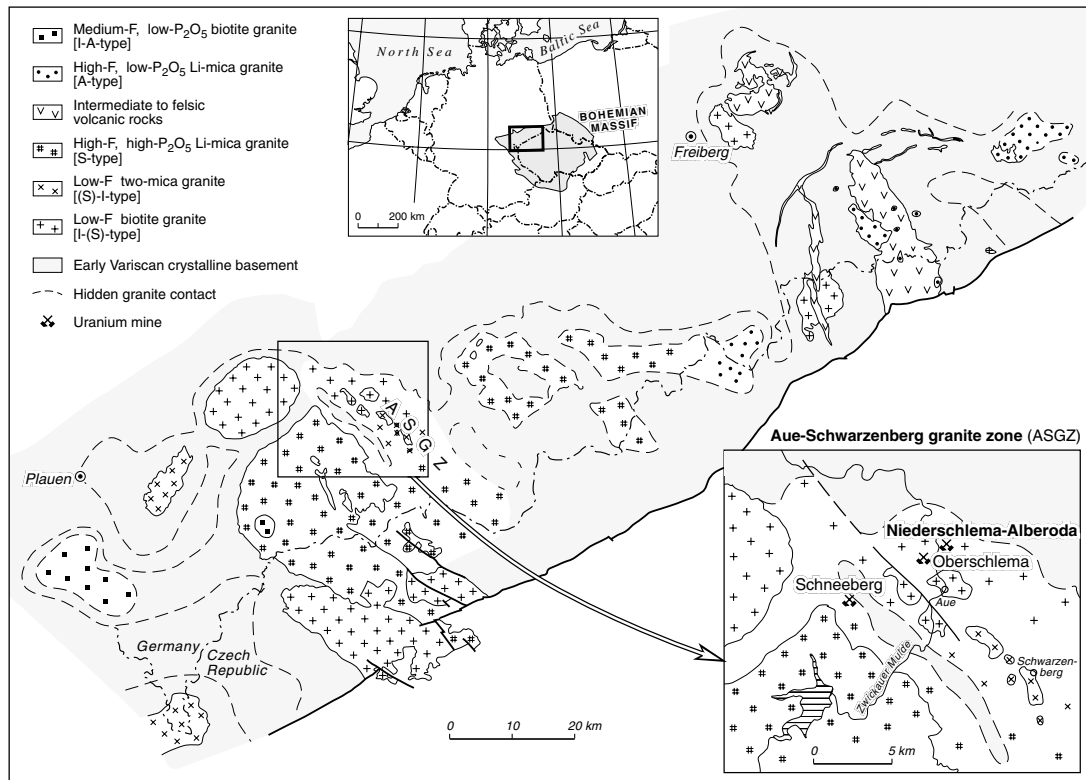


FIG. 1. Geological sketch-map, showing the location of the three uranium deposits forming the Schlema–Alberoda ore field and the distribution of the various groups of Variscan granites in the Erzgebirge.

petrovicite ( $\text{Cu}_3\text{HgPbBiSe}_5$ ; Johan *et al.* 1976) containing an excess of Bi, which, however, has not been approved by the IMA Commission on New Minerals and Mineral Names.

In the late 1990s, access to previously uninvestigated samples from both institutional and private collections encouraged the authors to undertake a further analytical campaign on the selenide minerals from this locality (Förster & Tischendorf 2001). Current results of this study include the discovery of a few compositionally unique grains representing solid solutions of the rare Se-bearing sulfosalts giraudite and hakite.

#### BACKGROUND INFORMATION

Giraudite (ideally  $\text{Cu}_{10}\text{Cu}_2\text{As}_4\text{Se}_{13}$ ) and hakite (ideally  $\text{Cu}_{10}\text{Cu}_2\text{Sb}_4\text{Se}_{13}$ ) are the Se-dominant analogues of the S-bearing minerals tennantite and tetrahedrite, respectively. By analogy with their S-dominant equivalents, and in consideration of compositional data available to date, the generalized formulae of a half unit-cell of the Se-bearing mineral family would be  $M^{+}_{10}M^{2+}_2X^{3+}_4Y^{2-}_{13}$ , where  $M^+$  represents Cu or Ag,  $M^{2+}$  represents Cu, Hg, Fe, Zn, and Cd,  $X$  stands for As and Sb, and  $Y$  comprises Se and S. Elements such as Pb, Mn, Bi, and Te, which are occasionally determined to be present in substantial abundances in the tetrahedrite–tennantite solid-solution series (*e.g.*, Johnson *et al.* 1986), have not been detected yet. On the other hand, Spiridonov *et al.* (1986) reported significant Tl (up to 2.56 wt%), Ge (up to 1.27 wt%) and Mo contents (up to 0.82 wt%) in hakite from Přeborčice, Czech Republic.

To date, giraudite has been reported only in association with uranium mineralization at Chaméane, France (Johan *et al.* 1982). Hakite has been described from three vein-type uranium deposits in the Bohemian Massif, Czech Republic: Přeborčice (Johan & Kvacek 1971, Brodin *et al.* 1981, Spiridonov *et al.* 1986), Bukov (Johan *et al.* 1978), and Petrovice (Johan 1989). Since the late 1980s, no further studies or new occurrences of either mineral have been reported.

Giraudite from Chaméane has the average composition ( $\text{Cu}_{9.41}\text{Ag}_{0.59}$ ) $_{\Sigma 10}$  ( $\text{Zn}_{1.09}\text{Cu}_{0.82}\text{Hg}_{0.06}\text{Fe}_{0.04}$ ) $_{\Sigma 2.01}$  ( $\text{As}_{2.32}\text{Sb}_{1.63}$ ) $_{\Sigma 3.95}$  ( $\text{Se}_{10.89}\text{S}_{2.15}$ ) $_{\Sigma 13.04}$  (cations normalized to 29 atoms per formula unit, *apfu*). Following the nomenclature for the tetrahedrite–tennantite solid-solution series, the mineral should be called a zincian giraudite. It contains up to 3.9 wt% Ag, 3.6% Zn, 4.1% S, and minor abundances of Hg (0.85%). Associated selenide minerals include clausthalite, bukovite, athabascite, umangite, berzelianite, klockmannite, eucairite, geffroyite, chaméanite, and eskebornite.

Hakite from Přeborčice is heterogeneous in composition. The type hakite is a mercurian hakite having an average composition of  $\text{Cu}_{10}(\text{Hg}_{1.85}\text{Cu}_{0.35})_{\Sigma 2.17}(\text{Sb}_{3.52}\text{As}_{0.63})_{\Sigma 4.15}(\text{Se}_{11.36}\text{S}_{1.31})_{\Sigma 12.67}$ ; it is associated with berzelianite, clausthalite, umangite, eskebornite, ferroselite, naumannite, tiemannite, eucairite, and

klockmannite (Johan & Kvacek 1971). Subsequent studies of mercurian hakite from this locality (Brodin *et al.* 1981, Spiridonov *et al.* 1986, Johan 1989) revealed the presence of significant Ag (up to 10.3 wt%) substituting for monovalent copper.

#### GEOLOGICAL AND MINERALOGICAL CONTEXT

Of the three uranium deposits forming the Schneeberg – Schlemma–Alberoda ore district (Schneeberg, Oberschlemma, Niederschlemma–Alberoda; Fig. 1), Niederschlemma–Alberoda, by far the largest, has produced ~80,500 tonnes of U prior to 1990 (*e.g.*, Lange *et al.* 1991). Between 1961 and 1995, mining activities focused on selenium took place at Niederschlemma–Alberoda, which is also the deposit richest in selenides. Such activities resulted in a total production of 1472 tonnes of selenium ore containing on average 0.52 wt% Se (Bunge 1999). It is also the deposit from which our sample containing the giraudite–hakite solid solution comes from. This sample was collected from the dike complex “Saar II”, at the –810-m level, gallery 23, near the main shaft (No. 371) located in the vicinity of the town of Hartenstein.

The uranium mineralization in the western Erzgebirge is spatially associated with F-poor but chemically evolved biotite granites (*e.g.*, Förster *et al.* 1999), which contain easily leachable Th-poor magmatic uraninite (Förster 1999). The formation of primary U-bearing veins took place during the early Permian (~270 Ma; Förster & Haack 1995, Förster 1996). Initially, uraninite crystallized with quartz, calcite, fluorite, coffinite, hematite, and sulfate minerals. During the Jurassic (~190 Ma), oxidizing hydrothermal solutions overprinted the veins and introduced new elements (Mg, Se, Pb, Ag), which probably were mobilized from the metamorphic country-rocks during fluid–rock interaction. During this event, Permian uraninite was destabilized, and the mobilized U was redeposited as another generation of spherical aggregates of uraninite accompanied by ankerite, dolomite, fluorite, hematite, and diverse selenide minerals. Hydrothermal activity in response to tectonic processes in the early Cretaceous (~120 Ma) again gave rise to alteration of earlier-formed mineral assemblages (Förster 1996). Pre-existing uraninite and selenide minerals were partially dissolved by the infiltrating fluids and replaced by Bi–Co–Ni arsenides and sulfides (Harlass & Schützel 1965). In addition to sulfides and remobilized uraninite and selenides, quartz, fluorite, barite, siderite, dolomite, and coffinite were deposited.

#### ANALYTICAL PROCEDURE

The ore assemblage was analyzed for Ag, Hg, Cu, Fe, Co, Ni, Zn, Cd, Pb, Pd, Pt, Sb, As, Bi, Te, S, and Se with an automated CAMEBAX SX–50 electron microprobe at the GeoForschungsZentrum Potsdam using wavelength-dispersion techniques. The operating con-

ditions were as follows: accelerating voltage 20 kV, beam current 40 nA, and beam diameter 1–2  $\mu\text{m}$ . The counting times on the peak were 30 s and, in each situation, half that time for background counts on each side of the peak. The data were corrected employing a PAP correction procedure (Pouchou & Pichoir 1985).

We used  $K\alpha$  lines for Fe, Co, Ni, Cu, Zn, Se, and S,  $K\beta$  lines for As,  $L\alpha$  lines for Hg, Pd, Pt, Cd, Sb, and Te,  $L\beta$  lines for Ag,  $M\alpha$  lines for Bi, and  $M\beta$  lines for Pb. Primary standards included pure metals for Co, Ag, Pd, and Pt, chalcopyrite for Fe, Cu, and S, pentlandite for Ni, sphalerite for Zn, cinnabar for Hg, galena for Pb, GaAs for As,  $\text{Bi}_2\text{Se}_3$  for Bi and Se,  $\text{Sb}_2\text{Te}_3$  for Te, InSb for Sb, and CdS for Cd.

In all mineral analyses, the concentrations of Pd and Pt were found to be below the detection limits.

## RESULTS

### *Petrographic description*

The Se-dominant sulfosalts are rare at Schlema-Alberoda. In the 22 polished sections examined in this study, they were observed only in one sample; in all, three anhedral grains of different size were observed, embedded in a dolomitic matrix. The largest grain, which is the subject of this paper, is about 330  $\mu\text{m}$  in length and 170  $\mu\text{m}$  in width (Fig. 2a). This member of the giraudite–hakite solid solution is closely associated with berzelianite, which occurs either in the interior or at the margin of the crystal and shows up in light purple in Figure 2a. Both minerals are accompanied by three small grains of galena, which show up best as yellow-green spots in the S-distribution map (Fig. 2e). Clausthalite forms the third selenide mineral present in the section.

### *Chemical composition*

Table 1 lists representative results of electron-microprobe analyses of the giraudite–hakite solid solution from Niederschlema–Alberoda, together with two compositions of Se-rich zincian tennantite from the same locality, previously described by Förster & Tischendorf (2001). Element correlations and compositional zoning are shown as X-ray element-distribution maps (Figs. 2, 3). Figure 2 displays the distribution of As, Sb, Hg, Se and S in the whole grain. Figure 3 is a close-up of the area marked by the inset box in Figure 2a. The abundances and ranges of various important elements in the giraudite–hakite structure are illustrated in Figure 4.

The complex internal zoning of the giraudite–hakite grain studied is most prominent in its distribution of Sb. The color scheme in Figures 2c and 3b reveals abrupt changes in Sb (and, consequently, in As also) during growth of the grain, with no apparent signs of a systematic pattern in terms of core–rim relations. Antimony in

concentrations corresponding to  $\geq 50$  mol% of the hakite component is only approached in those small areas appearing in yellow-green or yellow in Figures 2c and 3b. In contrast, Hg is more evenly distributed and shows no correlation with either As and Sb for most of the grain, except for the most As-enriched parts of the rim, where both cations display an inverse correlation (*cf.* Figs. 2b and 2d, and 3b and 3c, respectively). These areas do not show up at all in the Sb-distribution maps (Figs. 2c, 3a).

Copper is the dominant element among the monovalent species, accompanied only by minor amounts of Ag. Silver does not show any preference for either As or Sb and is consistently present at low concentrations between 0.07 and 0.36 wt%, which is equivalent to 0.01–0.08 atoms per formula unit (*apfu*).

The presence of Cu in excess of 10 *apfu* suggests that a small fraction of the copper occurs in the divalent state. The content of  $\text{Cu}^{2+}$ , determined by calculation, has previously been referred to as  $\text{Cu}^*$  (*e.g.*, Charlat & Lévy 1975, Johnson *et al.* 1986). Because no determination of charge was made,  $\text{Cu}^*$  was calculated accordingly;  $\text{Cu}^* = \text{Cu}_{\text{tot}} - (10 - \text{Ag}_{\text{tot}})$ . Even though  $\text{Cu}^*$  accounts for 0.08–1.10 *apfu*, Hg is usually the most prominent divalent element. Mercury is present at concentrations ranging from 9.0 to 15.4 wt%, which is equivalent to 0.97–1.81 *apfu* (Fig. 4a). Following the IMA rules for classification of the tetrahedrite–tennantite solid solutions, the selenide compositions refer to either mercurian giraudite or mercurian hakite, with one exception (*e.g.*, Table 1, anal. 1). Other minor divalent elements include Zn (0.15–0.28 wt%) and Fe (0–0.36 wt%). Lead, Co, and Ni are at or below their detection limits.

The concentrations of As and Sb vary considerably, As from 2.2 to 14.0 wt% (0.69–3.98 *apfu*), and Sb from 0.11 to 17.2 wt% (0.02–3.29 *apfu*) (Fig. 4b). In terms of mole percentages, As ranges from 17.4 to 99.5, and Sb ranges from 0.5 to 82.6. Sb-for-As substitution between giraudite and hakite seems complete. However, only a single composition represents the interval from 2.69 to 3.98 *apfu* As (or 0.7–1.38 *apfu* Sb).

Although Se is the main anion, S is consistently present at concentrations between 2 and 4 wt% (1.47–2.61 *apfu*) (Fig. 4c).

## DISCUSSION

### *Miscibility in the mercurian giraudite–hakite series*

Complete solid-solution between tetrahedrite and tennantite has long been established (*e.g.*, Johnson *et al.* 1986, Foit & Ulbricht 2001). Given their strong structural similarities, it is expected that complete substitution also should be possible between the giraudite and hakite end-members. The solid solutions studied in this paper span the range from  $\text{gir}_{99.5}\text{hak}_{0.5}$  to  $\text{gir}_{16.2}\text{hak}_{83.8}$ , almost free of compositional gaps. The identification of near-complete miscibility between two end-members in

TABLE 1. CHEMICAL COMPOSITION OF GIRAUDITE-HAKITE SOLID SOLUTIONS

Mineral	mercurian giraudite							mercurian hakite				zincian tennantite	
	Anal. No	1 <sup>a</sup>	2	3	4	5	6	7	8	9	10	11	12 <sup>b</sup>
Cu wt%	32.70	32.29	32.39	30.68	29.15	28.36	27.34	27.52	27.22	27.06	29.21	39.57	39.85
Ag	0.15	0.20	0.20	0.29	0.07	0.29	0.31	0.19	0.33	0.21	0.27	0.04	d.l.
Hg	8.97	9.39	9.48	12.48	14.20	14.65	15.32	14.98	14.88	14.73	9.89	d.l.	0.17
Zn	0.22	0.24	0.18	0.15	0.16	0.19	0.17	0.19	0.21	0.24	0.28	6.55	6.82
Cd												0.05	0.03
Fe	0.02	0.03	d.l.	0.03	d.l.	0.03	d.l.	0.03	0.02	0.02	d.l.	1.02	0.94
Co	d.l.	d.l.	d.l.	d.l.	d.l.	d.l.	d.l.	d.l.	0.02	d.l.	d.l.	d.l.	d.l.
Ni	d.l.	d.l.	d.l.	d.l.	d.l.	d.l.	d.l.	d.l.	d.l.	d.l.	d.l.	0.02	d.l.
As	14.02	13.80	13.76	12.16	8.72	7.91	6.90	6.23	4.28	3.01	2.23	17.82	18.21
Sb	0.19	0.32	0.26	2.67	7.42	8.01	9.68	10.36	13.81	15.06	17.17	0.54	0.34
Bi	d.l.	d.l.	d.l.	d.l.	d.l.	d.l.	d.l.	d.l.	d.l.	d.l.	d.l.	0.04	0.05
S	3.69	3.20	3.17	3.41	3.17	3.22	2.43	2.75	2.70	2.49	2.66	20.57	20.86
Se	39.08	39.98	39.98	38.34	37.37	37.35	37.73	37.55	37.01	37.08	37.54	13.97	12.96
Te												0.01	0.03
total	99.04	99.45	99.42	100.22	100.28	100.03	99.89	99.75	100.48	99.91	99.25	100.20	100.26
Cu	9.97	9.96	9.96	9.94	9.99	9.94	9.93	9.96	9.93	9.95	9.94	9.99	10.00
Ag	0.03	0.04	0.04	0.06	0.01	0.06	0.07	0.04	0.07	0.05	0.06	0.01	
sum $M^{+}$	10.00	10.00	10.00	10.00	10.00	10.00	10.00	10.00	10.00	10.00	10.00	10.00	10.00
Cu*	0.98	0.92	0.97	0.61	0.38	0.25	0.15	0.18	0.14	0.20	0.77	0.02	0.05
Hg	0.95	1.00	1.01	1.36	1.60	1.67	1.79	1.74	1.74	1.75	1.15		0.01
Zn	0.07	0.08	0.06	0.05	0.06	0.07	0.06	0.05	0.08	0.09	0.10	1.61	1.67
Cd												0.01	0
Fe	0.01	0.01		0.01		0.01		0.01	0.01	0.01		0.29	0.27
Co									0.01				
Ni												0.01	
sum $M^{2+}$	2.01	2.01	2.04	2.03	2.04	2.00	2.00	1.98	1.98	2.05	2.02	1.94	2.00
As	3.98	3.95	3.94	3.55	2.63	2.41	2.16	1.94	1.34	0.96	0.69	3.83	3.89
Sb	0.03	0.06	0.05	0.48	1.38	1.50	1.86	1.97	2.67	2.95	3.29	0.07	0.04
sum $Y^{3+}$	4.01	4.01	3.99	4.03	4.01	3.91	4.02	3.91	4.01	3.91	3.98	3.90	3.93
S	2.45	2.14	2.12	2.33	2.24	2.29	1.77	2.00	1.98	1.85	1.93	10.32	10.42
Se	10.53	10.84	10.86	10.61	10.70	10.80	11.20	11.10	11.02	11.20	11.07	2.85	2.63
sum $Z^{2-}$	12.98	12.98	12.98	12.94	12.94	13.09	12.97	13.10	13.00	13.05	13.00	13.17	13.05

blank: not analyzed, d.l.: detection limit, <sup>a</sup>: cuprian giraudite, <sup>b</sup>: from Förster & Tischendorf (2001),

Cu\* calculated as  $Cu_{tot} - (10 - Ag_{tot})$ .

one single grain only, as described here for giraudite and hakite from Niederschlema–Alberoda, is unique. Solid solutions narrowing the gap toward end-member hakite are known from Predborice, where recalculation of the microprobe data from Brodin *et al.* (1981) yields compositions approaching hak<sub>95</sub>gir<sub>5</sub> (Fig. 4b). These observations on natural phases provide good reasons to suggest the existence of a complete giraudite–hakite solid-solution series in nature, even though there is no experimental proof. However, strictly speaking, complete miscibility between the two selenides is only validated for solid solutions containing mercury as the predominant divalent cation. Complete substitution between the tetrahedrite–tennantite end-members is evident for solid solutions with Hg, Zn, or Fe fully occupying the  $M^{2+}$  position. No crystal-chemical reason is apparent to indicate that Hg rather than Zn, Fe, and Cu would extend the miscibility between giraudite and

hakite. Therefore, by analogy to their S-bearing equivalents, complete substitution between As and Sb should also occur in Hg-free giraudite–hakite under appropriate physicochemical conditions.

Previous studies of the selenide assemblage at Schlema–Alberoda revealed the presence of zincian tennantite containing 2.85 *apfu* Se (Förster & Tischendorf 2001). This composition represents the most Se-rich tetrahedrite–tennantite solid solution to date, including its tellurian end-member, goldfieldite (*e.g.*, Spiridonov & Okrugin 1985, Trudu & Knittel 1998). If this tennantite is plotted on a S *versus* Se diagram, together with all known giraudite–hakite compositions, the absence of solid solutions intermediate between tetrahedrite – tennantite – goldfieldite and giraudite–hakite is apparent (Fig. 4d). Mineral compositions between ~ 3 and 10 *apfu* S(Se) are not yet known. Galena and clausthalite are the only S- and Se-bearing end-members

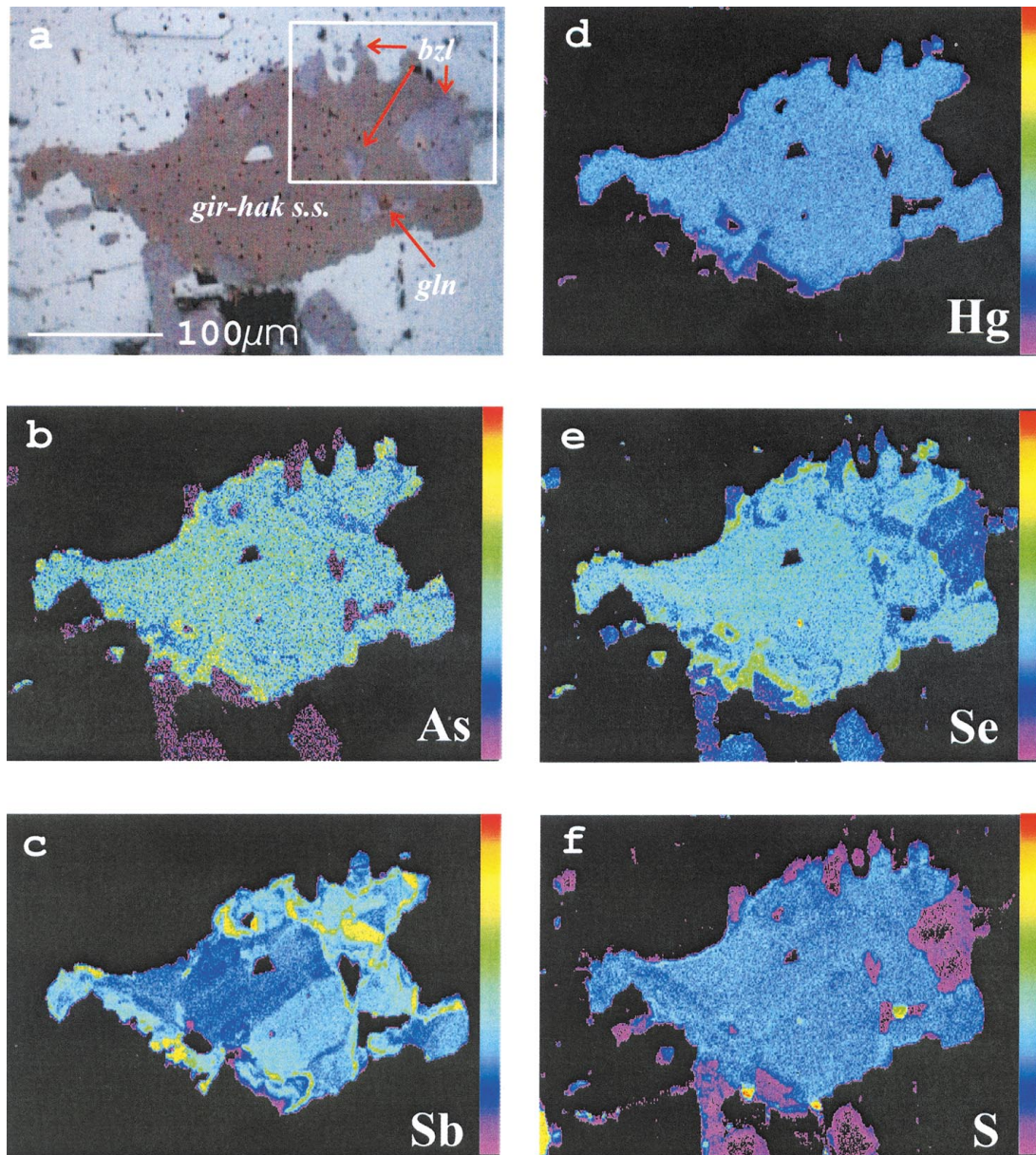


FIG. 2. Optical image (a) and X-ray elemental distribution maps for As (b), Sb (c), Hg (d), Se (e) and S (f) showing the internal zoning within the largest grain of giraudite-hakite found in this study. Symbols: bzl berzelianite, gln galena.

between which complete solid-solution has been demonstrated so far (Coleman 1959).

#### *Conditions of mineral formation*

Thermodynamic and experimental data are not yet available for giraudite and hakite, whether Hg-bearing

or not. These data would place important constraints on the stability of both phases. This poor state of knowledge precludes reliable inferences on the P-T-X conditions that prevailed during precipitation of these selenium-bearing minerals. Although information from fluid-inclusion studies is not available, Förster & Tischendorf (2001) estimated the following mineral-



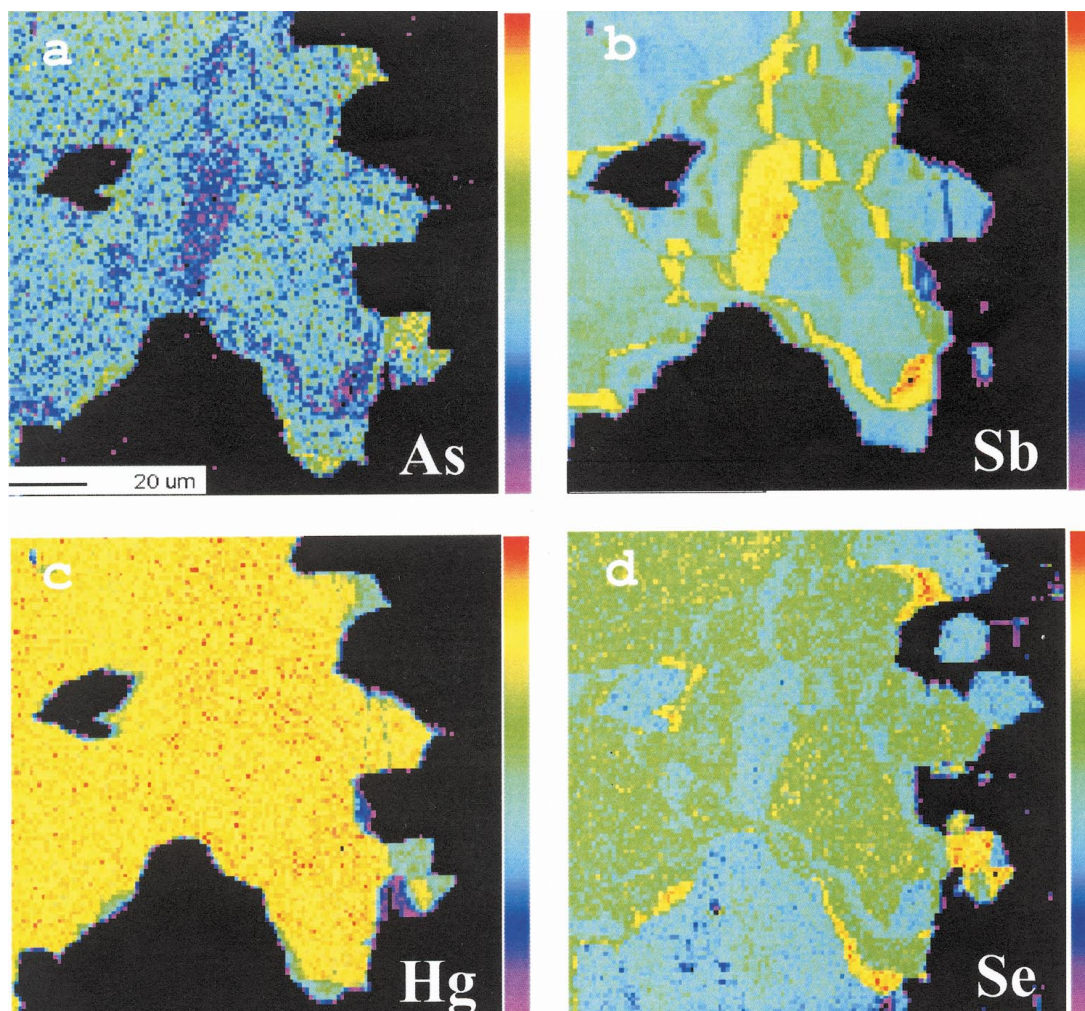


FIG. 3. Close-up of the area marked by the inset box in Figure 2, providing a more detailed insight into the distribution of As (a), Sb (b), Hg (c) and Se (d). Note that the images have been rotated 90° relative to those shown in Figure 2.

forming conditions for the main, Jurassic selenide stage at Schlemma–Alberoda, where umangite ( $\text{Cu}_3\text{Se}_2$ ) is a stable phase: 50–100 MPa, 100–150°C,  $-55 < \log f(\text{O}_2) < -50$ ,  $-12 < \log f(\text{Se}_2) < -15$ ,  $-26 < \log f(\text{S}_2) < -22$ ,  $f(\text{Se}_2)/f(\text{S}_2) > 1$ . Considering the absence of umangite and assuming that berzelianite ( $\text{Cu}_{2-x}\text{Se}$ ) and the giraudite–hakite solid solution are cogenetic, these conditions would not allow for precipitation of the Se-bearing phase. For the formation of berzelianite, a lower-temperature limit of ~110°C can be defined because at 112°C or below, berzelianite and high klockmannite ( $\beta\text{CuSe}$ ) would be expected to decompose into umangite (Chakrabarti & Laughlin 1981). An upper-T limit cannot be constrained because berzelianite

is stable up to more than 1000°C (*e.g.*, Simon & Essene 1996). Furthermore, berzelianite is stable over a wide range of  $f(\text{Se}_2)$ ,  $-14 < \log f(\text{Se}_2) < -30$  at 110°C according to the thermodynamic data presented by Simon *et al.* (1997). The rarity of tiemannite at Schlemma–Alberoda in general, and the absence of tiemannite in the selenide assemblage of the polished section in particular, suggest that the giraudite–hakite solid solution formed at Se fugacities below the HgSe–Hg univariant reaction [ $\log f(\text{Se}_2) < -20$  at 110°C], where berzelianite + hematite also form a stable assemblage. A lower limit of the Se fugacity is defined by the  $\text{Cu}_2\text{Se}$ –Cu univariant reaction [ $\log f(\text{Se}_2) \sim -31$  at 110°C]. Under these conditions, Hg would be free to enter the structure. A higher

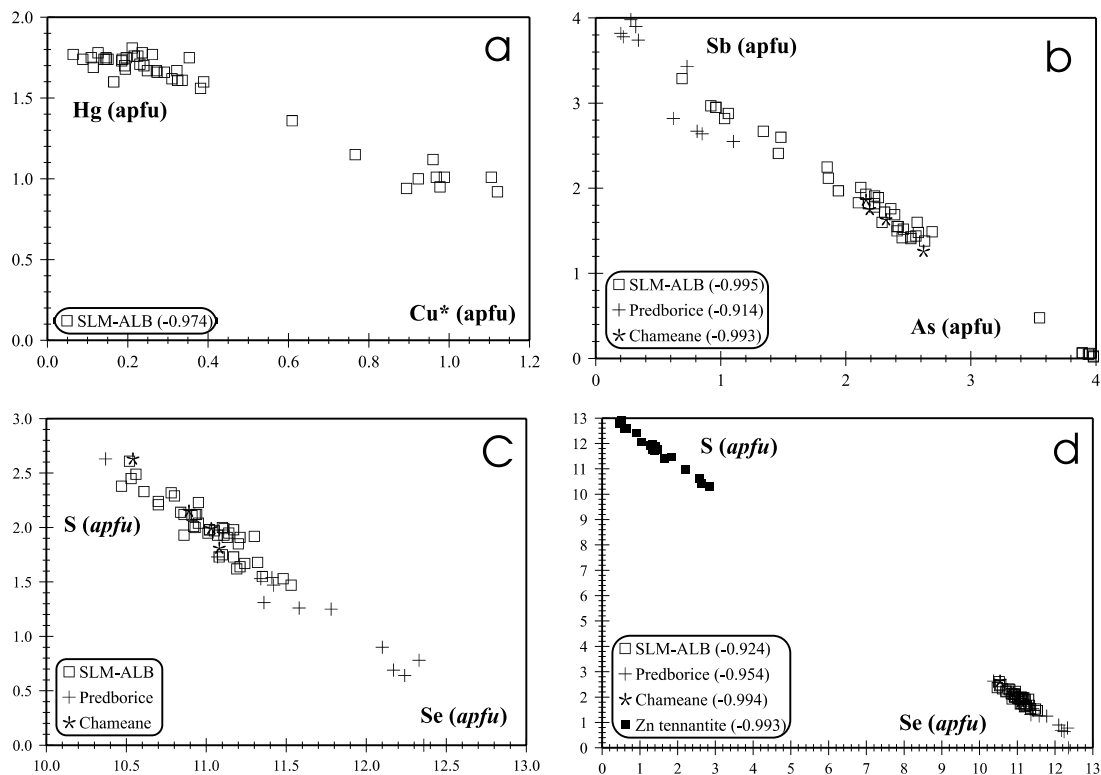


Fig. 4. Plots (in *apfu*) of Hg versus Cu\* (a), As versus Sb (b), and S versus Se (c, d) showing the extent of elemental substitutions in the giraudite–hakite solid solution from Niederschlema–Alberoda (SLM–ALB) and the other two known occurrences of these species. Also plotted in Figure 4d are the compositions of zincian tennantite from Niederschlema–Alberoda, studied by Förster & Tischendorf (2001). The correlation coefficient ( $r$ ) is given in parentheses.

temperature would shift  $\log f(\text{Se}_2)$  toward higher values. Berzelianite was identified as one of the earliest-formed selenides at Schlema–Alberoda (Förster & Tischendorf 2001), with an approximate temperature of crystallization of 150°C. According to this reconstruction, the origin of the Se-bearing mineral must have taken place early, when the Se activity in the fluid was not sufficiently high to crystallize tiemannite and Cu selenides other than berzelianite. Activities of Se as high as  $\log f(\text{Se}_2) \approx -12$  were approached in later stages of precipitation of selenide minerals and allowed umangite and klockmannite to form at temperatures below ~110°C. Thus, a comparatively low initial activity of selenium was likely responsible for the deposition of giraudite–hakite at some rare locations, and as it rose, further formation of giraudite–hakite was suppressed.

Given the lack of sulfides other than galena in the paragenesis, the activity of S also must have been low during precipitation of the Se mineral, likely below that defined by the reaction hematite + berzelianite = chalcocopyrite. At an oxygen fugacity corresponding to that

constrained by the magnetite–hematite buffer, this reaction would imply  $\log f(\text{S}_2)$  to be lower than –24 at  $T = 100^\circ\text{C}$  according to the thermodynamic dataset given by Simon *et al.* (1997). At this temperature, in the stability field of berzelianite, galena forms instead of claudthallite at  $\log f(\text{Se}_2)$  between –26 and –31 and  $\log f(\text{S}_2)$  between –24 and –28. Therefore, giraudite–hakite + berzelianite + galena may indeed represent an equilibrium assemblage.

Alternatively, the textural relations may be interpreted such that the Se mineral has replaced berzelianite. Destabilization of berzelianite during interaction with an Hg–As–Sb-bearing hydrothermal fluid may have provided the Cu and Se that were necessary to precipitate the giraudite–hakite solid solution. In this interpretation, the Se-bearing mineral presumably was deposited during the early Cretaceous, when the majority of the As was introduced into the system (*e.g.*, Harlass & Schützel 1965, Förster 1996). However, any inference on mineral age must remain tentative, given that minor amounts of As were probably present throughout the



entire evolution of the Schlema–Alberoda deposit. Moreover, this hypothesis appears to contradict the rarity of giraudite–hakite at Schlema–Alberoda. One would expect much more giraudite–hakite to have formed throughout the deposit, were a Hg–As–(Sb)-rich fluid introduced during a major ore-forming event.

The elemental zoning in the giraudite–hakite grain (Figs. 2, 3) imply strong fluctuations in the As/Sb activity ratio in the mineral-depositing fluid, whereas the activities of Hg and S did not vary significantly. However, the formation of tennantite instead of tetrahedrite (e.g., Table 1), as well as the volumetric predominance of giraudite over hakite, suggest that As was generally more important than Sb in the fluid phase forming the selenide mineralization at Schlema–Alberoda.

#### ACKNOWLEDGEMENTS

We thank Oona Appelt (GFZ Potsdam) for her assistance with the electron-microprobe work. The sample containing the giraudite–hakite grain was kindly provided by S. Flach (Damme, Germany) from his private collection (sample No. S 55). The comments and suggestions of two anonymous reviewers, as well as of Robert F. Martin and Franklin F. Foit Jr., helped to improve the substance of the paper.

#### REFERENCES

- BRODIN, B.V. (1967): Hydrothermal uraninite – coffinite – selenide associations. *Vop. Prikl. Radiogeol.* **2**, 195-219 (in Russ.).
- \_\_\_\_\_, OSIPOV, B.S., KACHALOVSKAYA, V.M., KOZLOVA, YE.V. & NAZARENKO, N.G. (1981): Silver-bearing hakite. *Int. Geol. Rev.* **23**, 71-73.
- BUNGE, W. (1999): Chronik der WISMUT. CD-Rom, WISMUT-GmbH, Chemnitz, Germany.
- CABRI, L.J., LAFLAMME, G.J.H., ROBERTS, A.C., CRIDDLE, A.H. & HULBERT, L.J. (1991): Jolliffeite and unnamed CoAsSe: two new arsenoselenides from the north shore of Lake Athabaska, Saskatchewan. *Can. Mineral.* **29**, 411-418.
- CHAKRABARTI, D.J. & LAUGHLIN, D.E. (1981): The Cu–Se (copper–selenium) system. *Bull. Alloy Phase Diagrams* **2**, 305-315.
- CHARLAT, M. & LÉVY, C. (1975): Influence des principales substitutions sur le paramètre cristallin dans la série tennantite – tétraédrite. *Bull. Soc. fr. Minéral. Cristallogr.* **98**, 152-158.
- COLEMAN, R.G. (1959): The natural occurrence of galena-clausthalite solid solution series [Colorado Plateau]. *Am. Mineral.* **44**, 166-175.
- \_\_\_\_\_, & DELAVALUX, M. (1957): Occurrence of selenium in sulfides from some sedimentary rocks of the western United States. *Econ. Geol.* **52**, 499-527.
- DILL, H. (1981): Zwei selenidführende Uranmineralisationen aus dem ostbayerischen Moldanubikum und ihre mögliche Bedeutung für die Klärung der Lagerstättengeneese. *Geol. Jahrb.* **D48**, 37-47.
- DYMKOV, YU.M., LOSEVA, T.I., ZAV'YALOV, YE.N., RYSHOV, B.I. & BOCHEK, L.I. (1982): Mgriite, (Cu,Fe)<sub>3</sub>AsSe<sub>3</sub>, a new mineral. *Int. Geol. Rev.* **25**, 859-863 [original: *Zap. Vses. Mineral. Obshchest.* **111**, 215-219 (in Russ.)].
- \_\_\_\_\_, RYZHOV, B.I., BEGIZOV, V.D., DUBAKINA, L.S., ZAV'YALOV, YE.N., RYAB'YEVA, V.G. & TSVETKOVA, M.V. (1991): Mgriite, Bi-petrovicite and associated selenides from carbonate veins of the Erzgebirge. In *New Data on Minerals* **37**. Izdatel'stvo Nauka, Moscow, Russia (81-101; in Russ.).
- \_\_\_\_\_, \_\_\_\_\_, ZAV'YALOV, YE.N., TSVETKOVA, M.V. & SHCHERBACHEV, D.K. (1989): Bi-variety of petrovicite from dolomitic veins of the Erzgebirge. *Dokl. Akad. Nauk SSSR* **306**, 1451-1455 (in Russ.).
- FOIT, F.F., JR. & ULBRICHT, M.E. (2001): Compositional variation in mercurian tetrahedrite – tennantite from the epithermal deposits of the Steens and Pueblo mountains, Harney County, Oregon. *Can. Mineral.* **39**, 819-830.
- FÖRSTER, B. (1996): *U/Pb-Datierungen an Pechblenden der U-Lagerstätte Aue–Niederschlema (Erzgebirge)*. Doctoral thesis, Justus-Liebig-Universität, Gießen, Germany.
- \_\_\_\_\_, & HAACK, U. (1995): U/Pb-Datierungen von Pechblenden und die hydrothermale Entwicklung der U-Lagerstätte Aue–Niederschlema (Erzgebirge). *Z. geol. Wiss.* **23**, 581-588.
- FÖRSTER, H.-J. (1999): The chemical composition of uraninite in Variscan granites of the Erzgebirge, Germany. *Mineral. Mag.* **63**, 239-252.
- \_\_\_\_\_, & TISCHENDORF, G. (2001): Se-rich tennantite and constraints on p–T–X conditions of selenide mineral formation in the Schlema–Alberoda uranium ore district (western Erzgebirge, Germany). *Neues Jahrb. Mineral., Abh.* **176**, 109-126.
- \_\_\_\_\_, \_\_\_\_\_, TRUMBULL, R.B. & GOTTESMANN, B. (1999): Late-collisional granites in the Variscan Erzgebirge, Germany. *J. Petrol.* **40**, 1613-1645.
- HARLASS, E. & SCHÜTZEL, H. (1965): Zur paragenetischen Stellung der Uranpechblende in den hydrothermalen Lagerstätten des westlichen Erzgebirges. *Z. angew. Geol.* **11**, 569-582.
- HARRIS, D.C., CABRI, L.J. & KAIMAN, S. (1970): Athabascaite: a new copper selenide from Martin Lake, Saskatchewan. *Can. Mineral.* **10**, 207-215.
- JOHAN, Z. (1989): Merenskyite, Pd(Te,Se)<sub>2</sub>, and the low-temperature selenide association from the Předbořice uranium deposit, Czechoslovakia. *Neues Jahrb. Mineral., Monatsh.*, 179-191.

- \_\_\_\_\_ & KVACEK, M. (1971): La hakite, un nouveau minéral du groupe de la tétraédrite. *Bull. Soc. fr. Minéral. Cristallogr.* **94**, 45-48.
- \_\_\_\_\_, \_\_\_\_\_ & PICOT, P. (1976): La petrovicite,  $\text{Cu}_3\text{HgPbBiSe}_5$ , un nouveau minéral. *Bull. Soc. fr. Minéral. Cristallogr.* **99**, 310-313.
- \_\_\_\_\_, \_\_\_\_\_ & \_\_\_\_\_ (1978): La sabatierite, un nouveau séléniure de cuivre et de thallium. *Bull. Minéral.* **101**, 557-560.
- \_\_\_\_\_, PICOT, P. & RUHLMANN, F. (1982): Evolution paragenétique de la minéralisation uranifère de Chaméane (Puy-de-Dôme), France: chaméanite, geffroyite et giraudite, trois séléniures nouveaux de Cu, Fe, Ag et As. *Tschermaks Mineral. Petrogr. Mitt.* **29**, 151-167.
- JOHNSON, N.E., CRAIG, J.R. & RIMSTIDT, J.D. (1986): Compositional trends in tetrahedrite. *Can. Mineral.* **24**, 385-397.
- LANGE, G., MÜHLSTEDT, P., FREYHOFF, G. & SCHRÖDER, B. (1991): Der Uranerzbergbau in Thüringen und Sachsen – ein geologisch-bergmännischer Überblick. *Erzmetall* **44**, 162-171.
- LEDENEVA, N.V. & PAKUL'NIS, G.V. (1997): Mineralogy and formation conditions of uranium–vanadium deposits in the Onega Depression, Russia. *Geol. Rudn. Mestorozhd.* **39**, 258-268 (in Russ.).
- POUCHOU, J.-L. & PICHOIR, F. (1985): "PAP" ( $\phi$ - $\rho$ - $Z$ ) procedure for improved quantitative microanalysis. In *Microbeam Analysis* (J.T. Armstrong, ed.). San Francisco Press, San Francisco, California (104-106).
- RUHLMANN, F., GILLET, Y. & LISSILLOUR, J. (1980): Une occurrence uranifère à sélénium et bismuth dans la ceinture métamorphique du leucogranite de Mortagne-sur-Sèvre (Vendée). *Bull. Minéral.* **103**, 245-249.
- RYSCHOW, B.I. (1972): Die "Braunspat"-Gänge des Sächsischen Erzgebirges (DDR) und die Stellung der in ihnen befindlichen Selenmineralisation. *Z. angew. Geol.* **18**, 149-157.
- SEELIGER, E. & STRUNZ, H. (1965): Erzpetrographie der Uran-Mineralien von Wölsendorf. II. Brannerit, Lermontovit (?), Selen und Selenide, Ni- und Bi-Begleitminerale etc. *Neues Jahrb. Mineral., Abh.* **103**, 163-178.
- SIMON, G. & ESSENE, E.J. (1996): Phase relations among selenides, sulfides, tellurides, and oxides. I. Thermodynamic properties and calculated equilibria. *Econ. Geol.* **91**, 1183-1208.
- \_\_\_\_\_, KESLER, S.E. & ESSENE, E.J. (1997): Phase relations among selenides, sulfides, tellurides, and oxides. II. Applications to selenide-bearing ore deposits. *Econ. Geol.* **92**, 468-484.
- SPIRIDONOV, E.M., KACHALOVSKAYA, V.M. & CHVILEVA, T.N. (1986): Thallium-bearing hakite, a new fahlore variety. *Dokl. USSR Acad. Sci., Earth Sci. Sect.* **290**, 206-208.
- \_\_\_\_\_, OKRUGIN, W.M. (1985): Selenium goldfieldite, a new variety of goldfieldite. *Dokl. USSR Acad. Sci., Earth Sci. Sect.* **280**, 476-478.
- TRUDU, A.G. & KNITTEL, U. (1998): Crystallography, mineral chemistry and chemical nomenclature of goldfieldite, the tellurian member of the tetrahedrite solid-solution series. *Can. Mineral.* **36**, 1115-1137.
- ZHENG, MINGHUA, LIU, JIAJUN & LU, WENQUAN (1993): The first discovery and preliminary study of selenio-sulfantimonide in China. *J. Mineral. Petrol.* **13**, 9-13 (in Chinese).

Received January 18, 2002, revised manuscript accepted June 4, 2002.